OXFORD
SOT | Society of Toxicology
academic.oup.com/toxsci

Toxicological Sciences, 2024, 1–12
https://doi.org/10.1093/toxsci/kfae058
Advance Access Publication Date: May 15, 2024
Research article

Downloaded from https://academic.oup.com/toxsci/advance-article/doi/10.1093/toxsci/kfae058/7674865 by UNIV OF TORONTO SCARBOROUGH LIBRARY user on 27 May 2024

The use of PD-1 functional knockout rats to study idiosyncratic adverse reactions to nevirapine

Tiffany Cho,[1] Anthony Hayes,[2] Jeffrey T. Henderson,[1] Jack Uetrecht[1,*]

[1]Leslie Dan Faculty of Pharmacy, Department of Pharmaceutical Sciences, University of Toronto, Toronto, Ontario M5S 3M2, Canada
[2]Department of Pathobiology, University of Guelph, Guelph, Ontario N1G 2W1, Canada

*To whom correspondence should be addressed at Leslie Dan Faculty of Pharmacy, Department of Pharmaceutical Sciences, University of Toronto, 144 College Street, Toronto, ON M5S 3M2, Canada. E-mail: jack.uetrecht@utoronto.ca

Abstract

Idiosyncratic drug reactions (IDRs) are associated with significant patient morbidity/mortality and lead to considerable drug candidate attrition in drug development. Their idiosyncratic nature makes the study of IDRs difficult. In particular, nevirapine is associated with a relatively high risk of serious skin rash and liver injury. We previously found that nevirapine causes a similar skin rash in female Brown Norway rats, but these animals do not develop significant liver injury. Programmed cell death protein-1 (PD-1) is an immune checkpoint involved in immune tolerance, and anti-PD-1 antibodies have been used to treat cancer. However, they increase the risk of liver injury caused by co-administered drugs. We found that PD-$1^{-/-}$ mice are more susceptible to drug-induced liver injury, but PD-$1^{-/-}$ mice are not a good model for all drugs. In particular, they do not develop a skin rash when treated with nevirapine, at least in part because they lack the sulfotransferase in their skin that forms the reactive metabolite responsible for the rash. Therefore, we developed a PD-1 mutant (PD-$1^{m/m}$) rat, with an excision in the ligand-binding domain of PD-1, to test whether nevirapine would cause a more serious skin rash in these animals. The PD-$1^{m/m}$ rat was based on a Sprague Dawley background, which has a lower incidence of skin rash than Brown Norway rats. The treated PD-$1^{m/m}$ rats developed more severe liver injury than PD-$1^{-/-}$ mice, but in contrast to expectations, they did not develop a skin rash. Functional knockouts provide a unique tool to study the mechanisms of IDRs.

Keywords: idiosyncratic drug reactions; adverse drug reactions; idiosyncratic drug-induced liver injury; skin rash; nevirapine; immune tolerance; PD-1; animal models

Idiosyncratic drug reactions (IDRs) are a significant source of patient morbidity and mortality. Moreover, they significantly increase the risk of failure during drug development because IDRs are usually encountered late in clinical trials or post-market surveillance when a large amount of money has already been invested in a drug candidate (Uetrecht, 2019; White *et al.*, 1999). Our understanding of IDRs is superficial, and without a better mechanistic understanding, it will be very difficult to predict or treat them. The unpredictable nature of IDRs makes them virtually impossible to study prospectively in patients. Animal models are important for mechanistic studies, but IDRs are also idiosyncratic in animals; therefore, valid animal models are rare (Uetrecht and Naisbitt, 2013).

Most animal models of IDRs involve acute toxicity and have very different characteristics from those of IDRs in humans. To be useful, an animal model must involve the same, or at least a very similar, mechanism as the IDR in humans. Therefore, the clinical characteristics should be very similar. In general, there is a delay between starting a drug and the onset of an IDR of weeks to months. This is typical of a delayed immune response, and there are also multiple lines of evidence to indicate that most IDRs are immune mediated (Cho and Uetrecht, 2017; Jee *et al.*, 2021; Sernoskie *et al.*, 2021). Mild IDRs are more common than serious IDRs, and the mild reactions often resolve despite continued treatment with the drug. If the IDR is immune-mediated and resolves despite continued treatment, the resolution must involve immune tolerance. We developed an animal model of amodiaquine-induced liver injury by using PD-$1^{-/-}$ mice co-treated with anti-CTLA-4 to impair immune tolerance. When treated with amodiaquine, these mice developed $CD8^+$ T-cell-mediated liver injury similar to the idiosyncratic drug-induced liver injury that amodiaquine can cause in humans (Mak and Uetrecht, 2015; Metushi *et al.*, 2015). This is consistent with the clinical observation that the use of checkpoint inhibitors increases the risk of IDRs caused by co-administered drugs (Ribas *et al.*, 2013). Idiosyncratic drug-induced liver injury is of much concern because it is a major IDR that leads to drug candidate failure (Jee *et al.*, 2021). Although the mouse PD-$1^{-/-}$ model is very useful, mice are not a good model for all IDRs, and we developed a rat with a targeted deletion of the PD-1 ligand-binding domain (within exon 2) using CRISPR (clustered regularly interspaced palindromic repeats)/Cas-9, which we will refer to as a PD-$1^{m/m}$ rat as previously described (Cho *et al.*, 2024). Similar to the PD-$1^{-/-}$ mouse, the PD-$1^{m/m}$ rat developed liver injury when treated with amodiaquine.

One test of the rat PD-$1^{m/m}$ model is with the use of nevirapine. Nevirapine, a potent non-nucleoside reverse transcriptase inhibitor for the treatment of HIV-1 infections, can cause a severe

© The Author(s) 2024. Published by Oxford University Press on behalf of the Society of Toxicology.
All rights reserved. For permissions, please e-mail: journals.permissions@oup.com

rash in patients (Bersoff-Matcha *et al.*, 2001; DrugBank, 2023). The skin rash has been observed in 3% of patients taking nevirapine in clinical trials. Moreover, women have a 7-fold increase in the risk of developing a severe rash. We also found that the treatment of rats with nevirapine caused an immune-mediated skin rash, which was strain- and sex-dependent (Shenton *et al.*, 2003). Specifically, the incidence was 100% in female Brown Norway rats, about 20% in female Sprague Dawley rats, 0% in female Lewis rats, and 0% in male rats of all the strains tested in the study. We found that nevirapine treatment in mice did not lead to a skin rash, at least in part, because they did not have the requisite sulfotransferase in the skin that is required to form the reactive metabolite responsible for the rash (Sharma *et al.*, 2013a). Nevirapine causes a wide variety of skin rashes in humans, the most serious being toxic epidermal necrolysis, which is mediated by $CD8^+$ T-cells (Friedmann *et al.*, 1994; Nassif *et al.*, 2004). The skin rash in the Brown Norway rat, although serious, appears to be mediated by $CD4^+$ T-cells (Shenton *et al.*, 2005). Blocking PD-1 promotes a $CD8^+$ T-cell response (Ahn *et al.*, 2018); therefore, it seemed likely that if we treated our PD-$1^{m/m}$ rats with nevirapine, it would result in an animal model that could be useful for the study of toxic epidermal necrolysis or Stevens-Johnson syndrome, 2 very serious skin rashes. We based the PD-$1^{m/m}$ model on Sprague Dawley rats because in previous experiments they had a low, but significant incidence of skin rash. If we had based it on Brown Norway rats, the rash might be worse, but it would be hard to show a difference because the incidence is already 100%, whereas if we used Lewis rats, there might be some reason that they are completely resistant because the incidence in previous experiments was zero.

Materials and methods

Animals

Rats with a targeted deletion of the PD-1 ligand binding domain were generated by CRISPR/Cas9 genome editing using pronuclear microinjection into Crl: CD(SD) Sprague Dawley embryos at the Model Production Core at the Centre for Phenogenomics (TCP; Toronto, Ontario, Canada) as described previously (Cho *et al.*, 2024). Female and male Sprague Dawley rats (3–4 months old) were bred in-house and maintained in the Canadian Council on Animal Care (CCAC)-accredited CCBR animal facility within the Division of Comparative Medicine at the University of Toronto (Toronto, Ontario, Canada). They were housed in pairs in standard cages in a 12-h light-dark (6:00 AM on/6:00 PM off) cycle with access to water and rodent meal *ad libitum*. Litters were weaned at 3 weeks and were ear-notched for genotyping purposes as previously described. Animals were then segregated by genotype (wild-type, heterozygous [PD-$1^{+/m}$], and homozygous deficient [PD-$1^{m/m}$]). In the 1–3-week studies, nevirapine (Boehringer-Ingelheim Pharmaceuticals, Ridgefield, Connecticut) was provided in a concentration of 0.2% w/w in Teklad global 18% rodent meal (2018; Harlan Laboratories; Indianapolis, Indiana), which was made by serial dilution of the drug with vigorous shaking and mixing. This concentration is equivalent to about 150 mg/kg body weight and produces a blood level in female rats within the therapeutic range in humans (Almond *et al.*, 2004; Chen *et al.*, 2008). Food and water were provided *ad libitum* to rats starting on day 0; control animals received regular rodent meals. Approximately 100 µl of blood was collected weekly *via* the tail vein using a 23G needle, which was repeated for the duration of the experiment (up to 3 weeks). Serum aminotransferase (ALT) levels were examined as a biomarker of liver injury. Whole blood was collected in Microvette capillaries with clot activator additive (CB300; Sarstedt; Nümbrecht, Germany) and centrifuged for 5 min at 11 200 × g. Using the ALT Liquid Stable Reagent (Thermo Scientific; Waltham, Massachusetts), ALT activity levels were determined as per package instructions. Body weights were recorded together with liver, spleen, thymus, and inguinal lymph node tissue weights at necropsy. Rats were euthanized at endpoint by CO_2 asphyxiation.

Animal Use Protocols were reviewed and approved by the Institutional Animal Care Committees, and all procedures followed the CCAC guidelines contained in the *Guide to Care and Use of Experimental Animals*, Vol. 1, second edition and CCAC *Guidelines on Transgenic Animals* (1997). Upon transfer to the Division of Comparative Medicine (CCBR Facility) at the University of Toronto, animal procedures were performed in accordance with the same guidelines outlined by the CCAC and approved by the Local Animal Care Committee.

RNA isolation and real-time polymerase chain reaction (qPCR)

Harvested tissues were washed in ice-cold phosphate-buffered saline (PBS) and immediately flash-frozen in liquid nitrogen. For liver RNA isolation, approximately 50 mg of frozen liver was homogenized in 500 µl of TRIzol Reagent (15596026; Thermo Fisher). Samples were incubated at room temperature to allow for the complete dissociation between complexes before the addition of chloroform. The samples were vigorously vortexed and centrifuged at 13 000 × g for 15 min at 4°C for phase separation. The upper aqueous phase was removed and mixed with an equal volume of 70% ethanol and transferred into RNA binding columns supplied by the Aurum Total RNA Mini Kit (7326820; Bio-Rad). The eluted RNA was collected and placed directly on ice. RNA concentration, purity, and quality were measured. Extracted liver RNA sample concentrations were adjusted to 50 ng/µl with the addition of DNase/RNase-free distilled water.

For the synthesis of cDNA, 10 µl of normalized RNA content was reverse-transcribed using SuperScript III Reverse Transcriptase and its components (18080044; Thermo Fisher). The reaction mixture consisted of 5× First Strand buffer, 0.1 mM dithiothreitol, 50 mM random hexamers (51-01-18-26; IDT), 10 µM dNTP mix (18427013; Thermo Fisher), SuperScript III Reverse Transcriptase, and distilled water in a total reaction volume of 20 µl per sample. Using the MJ Cycler Software 2.0 (Bio-Rad) on the Bio-Rad Chromo4 DyadDisciple, the cDNA synthesis reaction involved an initial 1-h incubation at 50°C followed by a 15-min enzyme inactivation step at 70°C. The synthesized reaction was then diluted with 60 µl of DNase/RNase-free distilled water. The qPCR reaction was prepared using SsoFast EvaGreen SYBR Supermix (172-5201; Bio-Rad), 10 µM each of the forward and reverse mRNA primer verified with NCBI Primer-BLAST (Bethesda, Maryland) for the gene of interest. Technical duplicates were performed for each target gene transcript and normalized to β-actin mRNA content. Reactions were performed with the following conditions: 95°C for 3 min for initial denaturation, 45 cycles of a series (95°C for 5 s for denaturation, 60°C for 20 s for extension), and held at 4°C upon completion. Data were analyzed using the Opticon Monitor 3 software (Bio-Rad) and fold changes were computed with the comparative cycle threshold (ΔΔCT) method and normalized to control wild-type animals.

Histology

The distal end of the left lateral lobe of the liver, a section of the spleen, both inguinal lymph nodes, and the thymus were

Downloaded from https://academic.oup.com/toxsci/advance-article/doi/10.1093/toxsci/kfae058/7674865 by UNIV OF TORONTO SCARBOROUGH LIBRARY user on 27 May 2024

collected at the endpoint. All samples were fixed in 10% neutral buffered formalin (Sigma-Aldrich), followed by embedding, sectioning (5 μm), and staining with hematoxylin/eosin. Slides were scanned using the Hamamatsu Nanozoomer 2.0 HT (20×) (Hamamatsu Photonics; Shizuoka, Japan) at the Princess Margaret Hospital HistoCore and the University of Toronto (Toronto, Ontario, Canada).

Flow cytometry

Liver mononuclear cells were isolated by digestion of minced whole liver in digestion buffer (1× PBS, 0.05% Type IV collagenase from *Clostridium histolyticum* [C0130; Sigma-Aldrich], 1.25 mM $CaCl_2$, 4 mM $MgSO_4$, 10 mM HEPES) for 30 min at 37°C. Spleen samples were processed similarly without the need for digestion. Contents were isolated through a 100-μm cell strainer, where 2–5 ml of anti-coagulant-citrate-dextrose buffer (1× PBS, 0.5% fetal bovine serum [FBS, F2242; Sigma-Aldrich], 0.6% citrate-dextrose solution [C3821; Sigma-Aldrich], 10 mM HEPES) was added and centrifuged at 30 × g for 3 min at 4°C. The supernatant was collected and centrifuged at 320 × g for 5 min at 4°C. The resulting pellet was resuspended with 2 ml RPMI buffer (1× RPMI-1640 medium [R0883; Sigma-Aldrich] 10% FBS, 10 mM HEPES) and layered on a 30% Percoll gradient (14 ml 1× PBS, 6 ml Percoll Centrifugation Media [17-0891-01; GE Healthcare, Chicago, Illinois]). For the isolation of peripheral blood mononuclear cells (PBMCs), whole blood was collected via cardiac puncture at endpoint and dispensed into EDTA blood collection tubes (368589; BD Biosciences, Franklin Lakes, New Jersey). Blood was rinsed with PBS, and the diluted sample was overlaid on Ficoll Paque Plus (GE Healthcare). Samples were centrifuged at 800 × g for 15 min with the brake turned off at 4°C. For PBMC collection, the buffy coat layer was harvested and washed with PBS. For all samples, the single cell pellet was resuspended with FACS buffer (1% FBS, 1× PBS) and counted with a hemocytometer stained with Trypan Blue (15250061; Thermo Fisher) where 10^7 of the live cells were plated per well.

All incubation steps in the staining procedure were conducted at room temperature and in the dark for 20 min. All concentrations used followed the supplier's recommendations. Centrifugation steps were set to 650 × g for 5 min at 4°C. To reduce Fc receptor-mediated binding by antibodies of interest to FcγII receptor-bearing cells for analysis, purified mouse anti-rat CD32 (550270; BD Biosciences) was preincubated with the cell suspension. Antibodies of interest were added directly to preincubated cells. Cells were characterized by staining with the following antibodies: BV421-conjugated anti-CD3 (563948; 1:40 dilution), BV605-conjugated anti-CD45RA (740372; 1:100 dilution), BV650-conjugated anti-CD161 (744052; 1:100 dilution), BV786-conjugated anti-CD8 (740913; 1:133 dilution), and BUV395-conjugated anti-CD4 (740256; 1:133 dilution) from BD Biosciences; eFluor506-conjugated Fixable Viability Dye (65-0866-14; 1:100 dilution), FITC-conjugated anti-FOXP3 (11-5773-82; 1:50 dilution), and PerCP-eFluor710-conjugated anti-CD25 (46-0390-82; 1:100 dilution) from Thermo Fisher; APC-conjugated anti-CD11b/c (201809; 1:40 dilution), APC/Cy7-conjugated CD45 (202216; 1:100 dilution), and PE/Cy7-conjugated anti-CD43 (202816; 1:40 dilution) from BioLegend (San Diego, California); and Alexa Fluor 700-conjugated anti-CD68 (MCA341A700; 1:50 dilution) from Bio-Rad. Helper T-cells were characterized as $CD3^+CD4^+$, cytotoxic T-cells as $CD3^+CD8^+$, macrophages as $CD68^+CD11b/c^+$; classical and non-classical monocytes as $CD11b/c^+CD43^-$, and $CD11b/c^+CD43^+$, respectively; T-regulatory cells (T_{reg}) cells as $CD3^+CD4^+CD25^+FOXP3^+$; NK cells as $CD3^-CD161^+$; NKT cells as $CD3^+CD161^+$; dendritic cells as $CD11b/c^+MHCII^+$; and B-cells as $CD3^-CD45RA^+$. For intracellular staining, the FOXP3/Transcription Factor Staining Set (00-5523-00; Thermo Fisher) was used according to the manufacturer's instructions. Cells were counted on a BD LSR Fortessa X-20 Cell Analyzer (BD Biosciences) using FACSDiva for data acquisition. Data analysis was conducted on FlowJo 10 software (Tree Star Inc., Ashland, Oregon). For flow cytometry analysis, cells were initially gated on singlets (FSC-H vs FSC-A), live cells, and then by population. A minimum of 50 000 cells/sample were acquired for each analysis.

Statistical analysis

All data were presented as the means ± standard error of the mean (SEM). One-way or 2-way analysis of variance (ANOVA) followed by Tukey's *post-hoc* test was used to assess for statistical significance (* or † denotes $p < .05$ for a treatment-mediated effect or a genotype-mediated effect, respectively) using GraphPad Prism 6 (San Diego, California).

Results

Treatment with nevirapine did not lead to a skin rash; however, it did lead to increased moribundity and mortality in treated PD-1$^{m/m}$ rats

It was hypothesized that the incidence and severity of nevirapine-induced skin rash would be increased by deletion of the PD-1 ligand binding domain, and it might also lead to an increased sensitivity to nevirapine-induced liver injury (Figure 1). In contrast to previous studies in which about 20% of wild-type female Sprague Dawley rats treated with nevirapine developed a rash (Shenton *et al.*, 2003), none of the wild-type or PD-$1^{m/m}$ rats of either sex developed a rash in the current study (Supplementary Figure 1). Female nevirapine-treated PD-$1^{m/m}$ rats became ill with heavy porphyrin staining around the nose and eyes, orbital tightening, hunched posture, respiratory distress, ungroomed fur, and animals were cold to the touch. Death and early termination due to moribundity occurred at ≤3 weeks. Similarly, nevirapine-treated PD-$1^{m/m}$ males were euthanized between 4–5 weeks (inclusive) due to multiple features of distress. Moribundity or premature mortality was not observed in any nevirapine-treated wild-type animals.

Treatment with nevirapine led to significant increases in liver weights in treated female PD-1$^{m/m}$ rats but increases in spleen and inguinal lymph node weights in the nevirapine-treated PD-1$^{m/m}$ rats of both sexes

Liver lobes in the treated female PD-$1^{m/m}$ rats were often grossly abnormal with lesions and/or areas with discoloration (Supplementary Figure 2). The spleens and inguinal lymph nodes were visibly larger in the treated PD-$1^{m/m}$ animals in comparison to treated wild-type animals (Supplementary Figure 2). Treated PD-$1^{m/m}$ females had increased liver weights at day 14, which was significantly greater than the liver weights of control PD-$1^{m/m}$ females or nevirapine-treated wild-type females (Figure 2). On day 21, the difference in female liver weights between the treated wild-type and PD-$1^{m/m}$ animals was abolished, but there were significant increases in the treated animals compared with untreated controls. Consistent with the images of the enlarged spleen and inguinal lymph nodes, nevirapine-treated PD-$1^{m/m}$ females had a significantly larger spleen weight on days 14 and 21. These animals also had larger inguinal lymph nodes on days 7,

Downloaded from https://academic.oup.com/toxsci/advance-article/doi/10.1093/toxsci/kfae058/7674865 by UNIV OF TORONTO SCARBOROUGH LIBRARY user on 27 May 2024

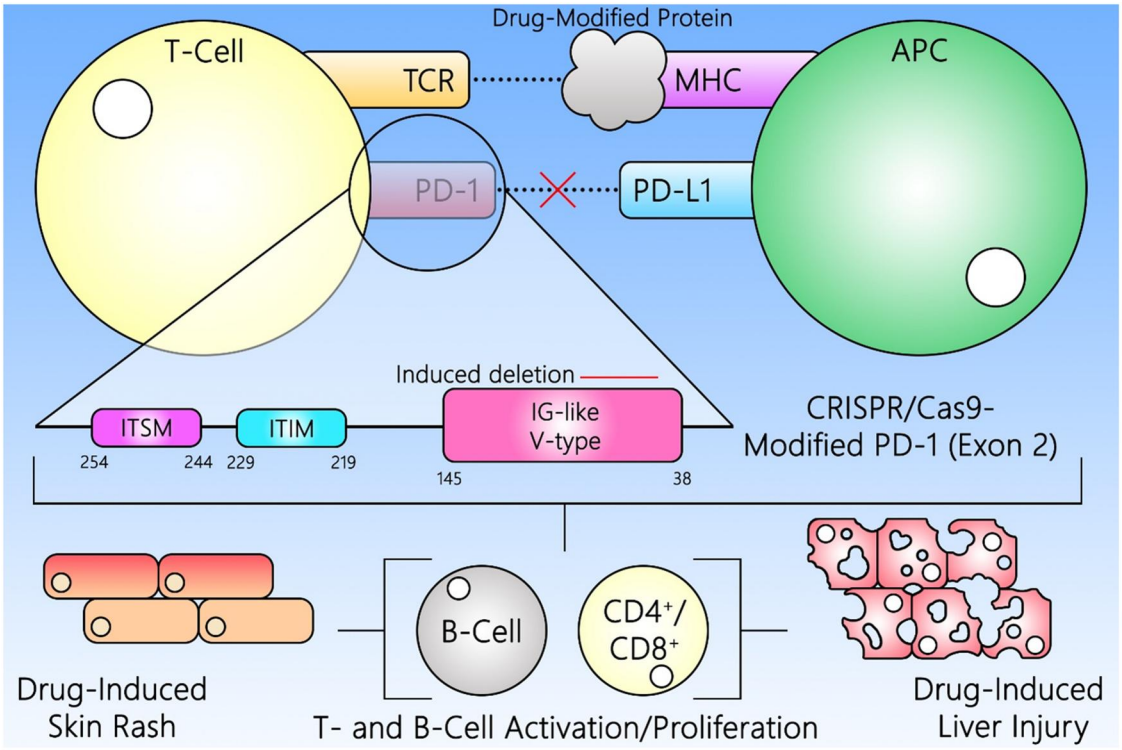

Figure 1. PD-1 is involved in immune tolerance, and it was hypothesized that deletion of the PD-1 ligand binding domain would increase the incidence and severity of immune-mediated nevirapine-induced skin rash and liver injury. This deletion was accomplished through a CRISPR/Cas9-mediated deletion of a segment of exon 2 of the rat *PDCD1* gene. (TCR, T-cell receptor; MHC, major histocompatibility complex; APC, antigen-presenting cell).

14, and 21. A significant decrease in thymus weights was observed at day 21 in the nevirapine-treated animals and also in the untreated PD-$1^{m/m}$ animals (Figure 2). Because major body weight changes were observed closer to the end of the experiment, that is, day 21 for females or when animals began displaying signs of moribundity, and day 35 for the males, that is when they were weighed (Supplementary Figure 3). Tissue weights in male rats were weighed at day 35 (endpoint) only. In comparison with the females, nevirapine-treated PD-$1^{m/m}$ males had significantly increased spleen and inguinal lymph node weights (Supplementary Figure 4). Although the increased liver weights observed in nevirapine-treated PD-$1^{m/m}$ females were not observed in males, there was a non-significant trend of increased tissue weights in treated wild-type and PD-$1^{m/m}$ males. Although there was a trend toward a decreased thymus weight in nevirapine-treated PD-$1^{m/m}$ males, no significant differences were detected.

Histology of the liver, spleen, and lymph nodes reveal cellular and morphological changes in nevirapine-treated PD-$1^{m/m}$ rats

Diffuse hepatitis with a marked depletion of hepatocytes and active necrosis/apoptosis was seen in the liver of nevirapine-treated PD-$1^{m/m}$ females. Mononuclear leukocyte infiltrates were also present surrounding the central vein and periportal areas. Overall, there was widespread disorganization of hepatocytes with prominent diffuse interstitial leukocytic infiltration and apoptotic hepatocytes in the liver of the nevirapine-treated PD-$1^{m/m}$ females (Figure 3). In the spleen of the nevirapine-treated wild-type females during the third week and nevirapine-treated PD-$1^{m/m}$ females throughout treatment, extensive areas of extramedullary hematopoiesis (EMH) were also present in the red pulp, with a few intact lymphoid areas in the periarteriolar sheaths and adjacent follicles (Figure 4). Large areas of follicular dissociation and ablation were apparent in the nevirapine-treated PD-$1^{m/m}$ females, which worsened throughout treatment. The inguinal lymph nodes in the nevirapine-treated females showed fewer primary and secondary follicles than in control animals, which became unidentifiable later in treatment (Supplementary Figure 5). At day 35, similar patterns of leukocytic infiltration near the central vein and periportal areas were present in the nevirapine-treated PD-$1^{m/m}$ males with some hepatocellular necrosis/apoptosis (Supplementary Figure 6). The zones between the red pulp and white pulp in the spleen were slightly less distinguishable in the spleen of the treated PD-$1^{m/m}$ males. Similar to the nevirapine-treated PD-$1^{m/m}$ females at endpoint, the follicular structures within the lymph nodes were distorted by day 35 in the nevirapine-treated males.

Flow cytometry of the leukocytic cells in the liver, spleen, and blood indicate significant changes in cell populations

Eleven populations of single cells were quantified by flow cytometry in the liver, spleen, and blood to determine the cellular changes in these tissues at different time points (Supplementary Figure 7). Immunophenotyping was conducted on days 7, 14, and 21 (Figure 5) in the females and on day 35 in the males (Supplementary Figure 8). In the liver, a significant increase in cytotoxic T-cells in the nevirapine-treated PD-$1^{m/m}$ females appeared as early as day 7 and remained elevated on days 14 and 21 (Supplementary Figs. 9 and 10). The relative decrease in T-helper cells and B-cells in the liver of nevirapine-treated PD-$1^{m/m}$ females was also sustained from the earliest time point to day 21. Similarly, a significant increase in cytotoxic T-cells was observed in the nevirapine-treated PD-$1^{m/m}$ males with a relative

Downloaded from https://academic.oup.com/toxsci/advance-article/doi/10.1093/toxsci/kfae058/7674865 by UNIV OF TORONTO SCARBOROUGH LIBRARY user on 27 May 2024

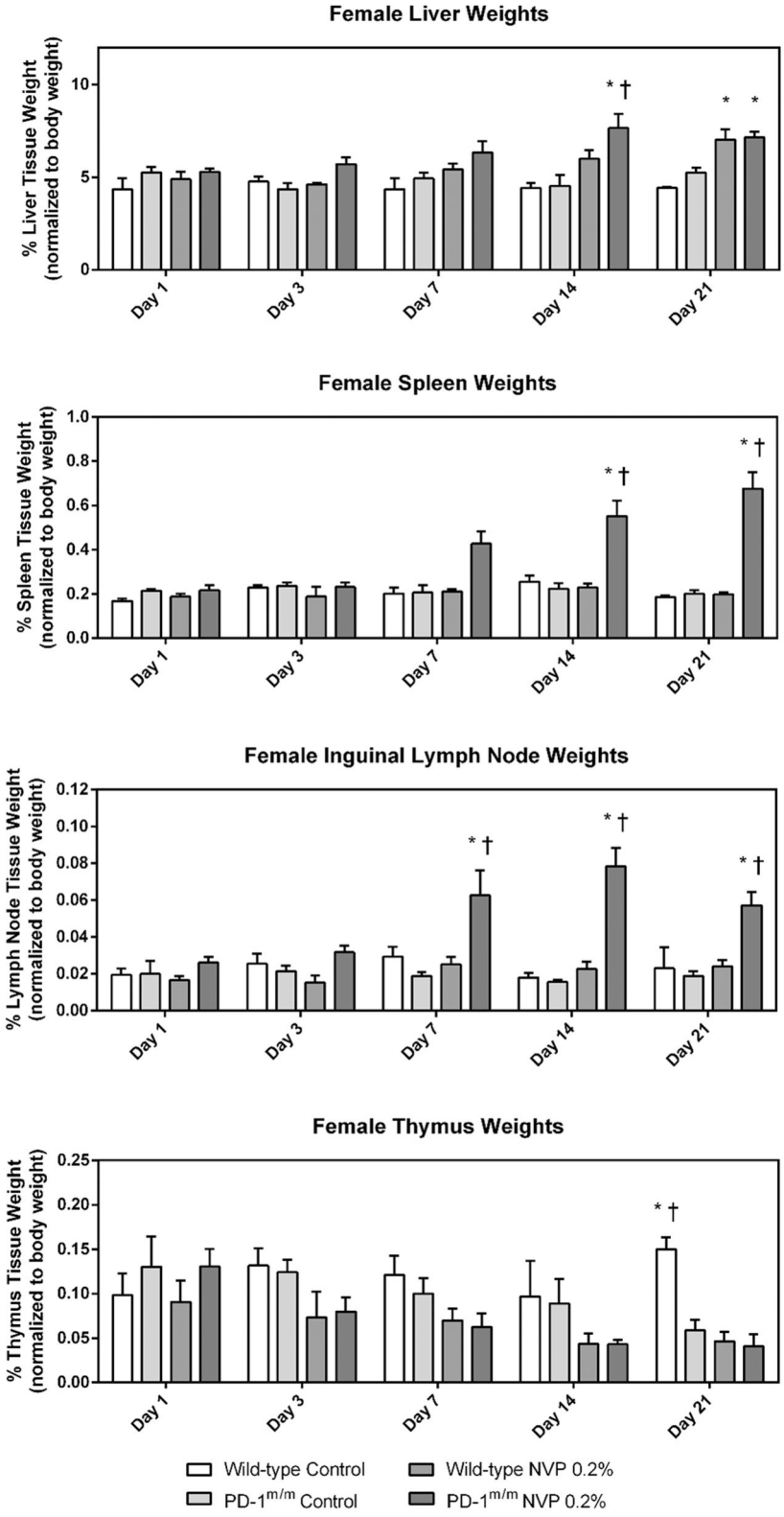

Figure 2. Weight of the whole liver, spleen, inguinal lymph nodes, and thymus in control and treated wild-type and PD-1$^{m/m}$ female rats at endpoint (day 21). Liver: At day 14, nevirapine (NVP)-treated PD-1$^{m/m}$ females were observed with an increased liver weight compared with treated wild-type females and control PD-1$^{m/m}$ animals. On day 21, both treated wild-type and PD-1$^{m/m}$ groups had increased liver weights compared with their control counterparts. Spleen: On days 14 and 21, nevirapine-treated PD-1$^{m/m}$ females had significantly increased spleen weights compared with treated wild-type females and control PD-1$^{m/m}$ animals. No other trends or changes were observed. Inguinal lymph nodes: On days 7, 14, and 21, nevirapine-treated PD-1$^{m/m}$ females had significantly increased inguinal lymph node weights compared with treated wild-type females and control PD-1$^{m/m}$ animals at each respective time point. No other trends or changes were observed. Thymus: At day 21, all treated and control PD-1$^{m/m}$ females had significantly decreased thymus weights when compared with control wild-type animals. Data were normalized to individual body weights at endpoint. Data were normalized to individual body weights at endpoint. The data represent the mean ± SEM, and statistical significance was tested using a 2-way ANOVA with Tukey's multiple comparisons test ($n = 3$–19 per group), * $p < .05$ for treatment-mediated effects between control and nevirapine treatments (same genotype, different treatment); † $p < .05$ for genotype-mediated effects between wild-type and PD-1$^{m/m}$ animals (same treatment, different genotype).

Downloaded from https://academic.oup.com/toxsci/advance-article/doi/10.1093/toxsci/kfae058/7674865 by UNIV OF TORONTO SCARBOROUGH LIBRARY user on 27 May 2024

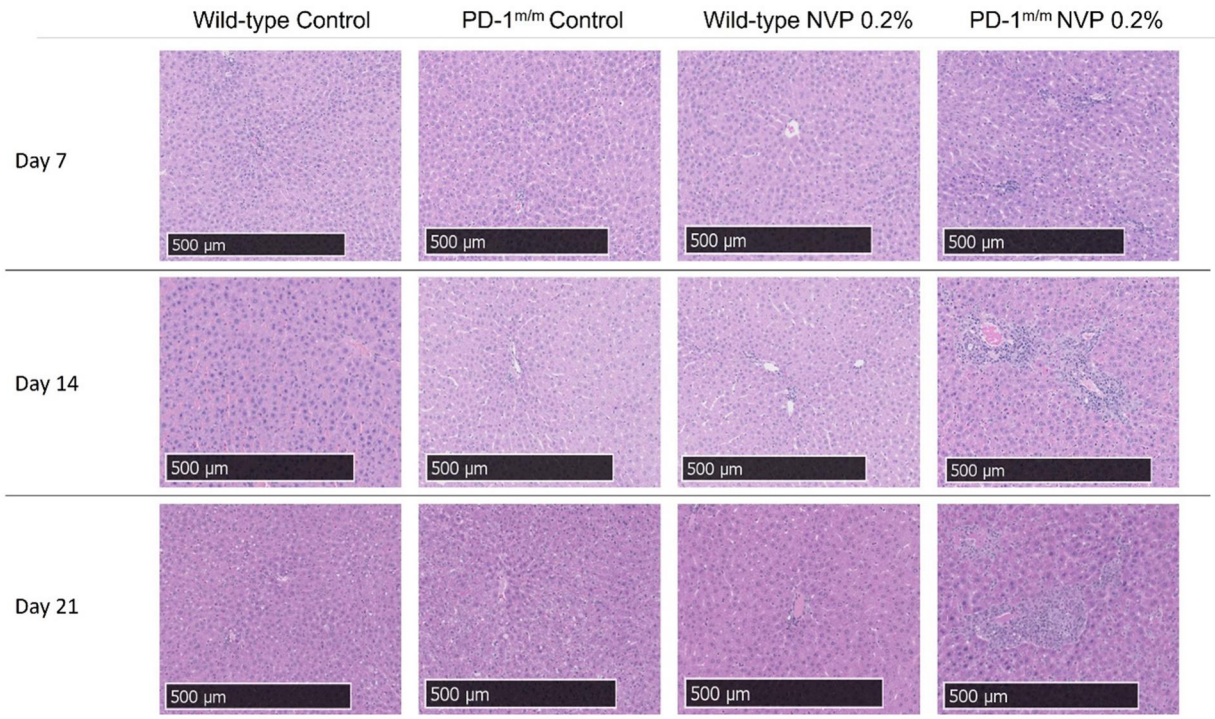

Figure 3. H&E-stained liver sections from the left lateral lobe in female rats at endpoint (days 7, 14, and 21). The architecture and cellularity of the control groups appeared undisturbed; however, focal areas of inflammation were observed in the 2- and 3-week nevirapine (NVP)-treated wild-type (WT) females. Areas of marked hepatocyte depletion and active necrosis/apoptosis were observed in the nevirapine-treated PD-1$^{m/m}$ females with increasing severity over time. Representative images are shown at 5× magnification.

decrease in T-helper cells and B-cells in the liver. The fraction of dendritic cells was also significantly lower on day 35 in the males. Consistent throughout the study, a relative decrease in B-cells was observed in the spleen of the nevirapine-treated PD-1$^{m/m}$ animals. A relative decrease in T-helper cells was also apparent on day 7 and day 21, but not on day 14. The only cellular increases in the spleen of the nevirapine-treated PD-1$^{m/m}$ animals were present on day 7 with elevations in cytotoxic T-cells, NK cells, NKT cells, and non-classical monocytes (Supplementary Figure 9). In males, only a relative decrease in B-cells was observed in the spleen of the nevirapine-treated PD-1$^{m/m}$ animals (Supplementary Figure 8). In the blood, increases in cytotoxic T-cells were detected on days 7, 14, and 21 in the female nevirapine-treated PD-1$^{m/m}$ rats and on day 35 in the nevirapine-treated PD-1$^{m/m}$ males. Along with the increase in cytotoxic T-cells, NKT cells were also significantly elevated when compared with nevirapine-treated wild-type females on day 7, with increases in NK cells and classical monocytes on day 14 and day 21. A decrease in T-helper cells and B-cells was present on days 7 and 21, and although a decreased trend can also be observed on day 14, it was not significant.

Nevirapine treatment led to increased gene expression of inflammatory cytokines and chemokines in the liver

mRNA primer sequences are presented in Supplementary Table 1. Significant increases in TNFα, IL-1β, IL-18, TGFβ1, CCL2, and CCL3 transcript levels were observed in the nevirapine-treated PD-1$^{m/m}$ females, and these increases were greater in comparison with nevirapine-treated wild-type or control PD-1$^{m/m}$ females (Figure 6). An increase in PD-L1 mRNA levels was also observed. Although there was a trend toward an increase in IL-17A levels in the nevirapine-treated PD-1$^{m/m}$ females, this was not statistically significant. An increase in ARG1 mRNA levels was also noted in the nevirapine-treated wild-type females in comparison with all other groups.

PD-1 exon 2 modification promotes alternative splicing

Prior CRISPR-mediated gene modification has demonstrated the potential for relatively benign modifications (point mutations) to induce changes in gene splicing (Zhang *et al.*, 2020). In addition, the wild-type PD-1 transcripts have previously been suggested to be capable of undergoing alternative splicing of exons 2 and 3 (Nielsen *et al.*, 2005). With this in mind, we examined relative levels of exon expression in wild-type and PD-1$^{m/m}$ rats using real-time qPCR with primers designed to detect PD-1 mRNA transcript changes in the liver in the presence of drug treatment with nevirapine and normalized to β-actin expression levels using primers shown in Supplementary Table 2. As shown in Figure 7, the induced deletion within exon 2 results in a substantial depression in exon 2 utilization. In addition, this alteration results in a relative enhancement in exon 1 and exon 3–5 expression in PD-1$^{m/m}$ females compared with wild-type animals. Within exons 3–5, a 12-fold increase was detected in the nevirapine-treated animals when compared with untreated PD-1$^{m/m}$ animals and nevirapine-treated wild-type animals.

Nevirapine-treated PD-1$^{m/m}$ females developed delayed-onset liver injury

By day 14 and day 21, increases in serum ALT levels in the nevirapine-treated PD-1$^{m/m}$ rats were significant compared with nevirapine-treated wild-type and control PD-1$^{m/m}$ females (Figure 8). In the males, serum ALT levels peaked at day 14 and the level of injury appeared to decline over time, and differences between groups were negligible on day 35. Significant increases in total serum bilirubin were observed in the nevirapine-treated

Downloaded from https://academic.oup.com/toxsci/advance-article/doi/10.1093/toxsci/kfae058/7674865 by UNIV OF TORONTO SCARBOROUGH LIBRARY user on 27 May 2024

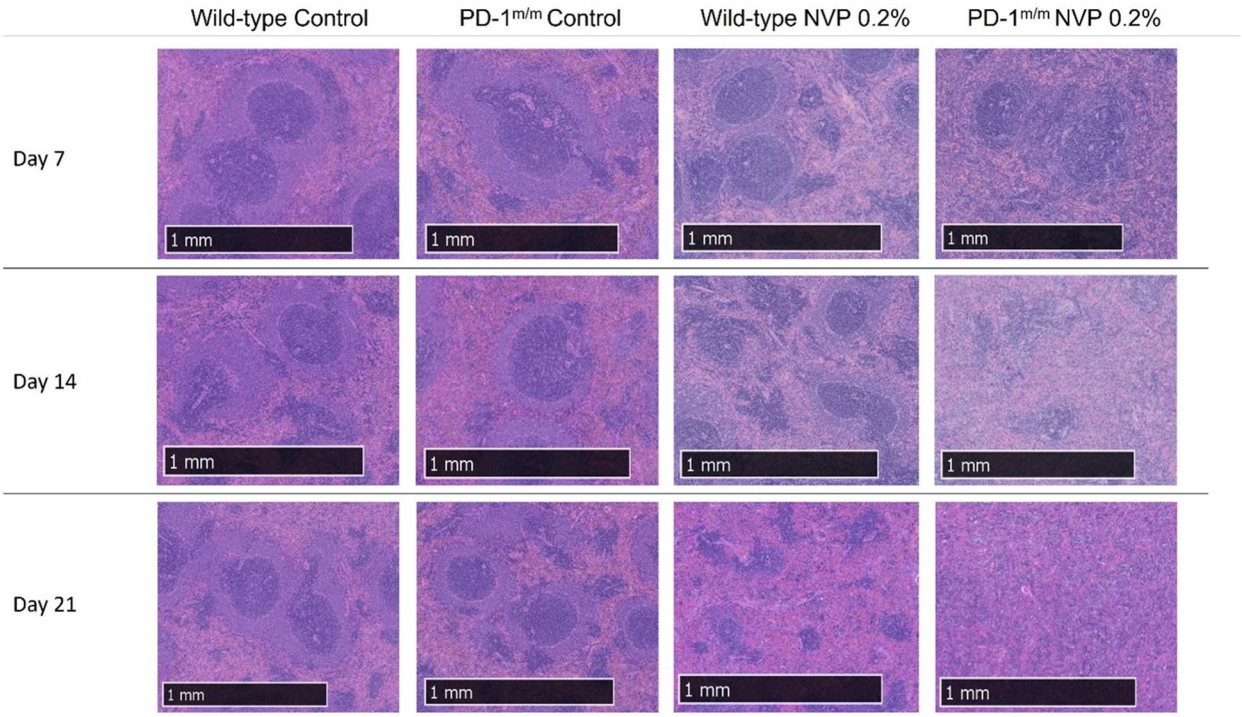

Figure 4. H&E-stained spleen sections were taken from the distal ends in female rats at endpoint (days 7, 14, and 21). White pulp atrophy was apparent with the disorganization of the lymphoid follicles and marginal zones at week 3 in the nevirapine (NVP)-treated wild-type (WT) females and week 1 in the nevirapine-treated PD-$1^{m/m}$ females. At weeks 2 and 3, the follicles were completely abolished and absent in the nevirapine-treated PD-$1^{m/m}$ females. Representative images are shown at 2.5× magnification.

PD-$1^{m/m}$ females on day 23 (Figure 9), which complement the similar increases in serum ALT activity levels.

Age may be a risk factor for increased liver injury

To determine if age was a presiding factor in eliciting greater levels of liver injury, nevirapine-treated wild-type and PD-$1^{m/m}$ females of different ages (3–12 months) were used (Supplementary Figure 11). Females were only observed in this instance as they appeared to be more sensitive to delayed-onset drug-induced liver injury. As each data point is a single rat, statistics were not used to determine the significance of the data. However, 12-month-old nevirapine-treated PD-$1^{m/m}$ females appear to have an increasing trend in serum ALT levels compared with younger PD-$1^{m/m}$ females.

Heterozygous females are phenotypically similar to wild-type females with respect to their extent of liver injury and measured serum cholesterol levels

Heterozygous females were treated with nevirapine to determine their phenotype in response to the drug-induced liver injury in comparison with wild-type animals (Supplementary Figure 12). Females were only observed in this instance as PD-$1^{m/m}$ females appeared to be more sensitive to nevirapine treatment. No differences were detected between the nevirapine-treated heterozygous and wild-type females, but significant increases in the nevirapine-treated PD-$1^{m/m}$ females were detected on day 22. Moreover, cholesterol was measured in female wild-type, heterozygous, and PD-$1^{m/m}$ animals as cholesterol homeostasis is largely impaired in liver disease and can result in a decrease in circulating cholesterol levels in the serum (Chrostek *et al.*, 2014). On day 14 and day 21, the total serum cholesterol levels were unchanged in wild-type and heterozygous females; however, significant decreases were observed in the nevirapine-treated PD-$1^{m/m}$ females (Supplementary Figure 13).

Discussion

Mechanistic studies of IDRs are very difficult. In general, IDRs are characterized by a delay between starting a drug and the onset of the IDR. It is important to understand the events leading up to an IDR, but given the unpredictable nature of these adverse reactions, it is impossible to study patients prospectively. The immune system is extremely complex and involves many different types of cells in multiple locations, which is impossible to duplicate *in vitro*. Therefore, we are left with trying to develop animal models, and even failures can provide additional mechanistic clues.

We previously found that the impairment of immune tolerance by blocking immune checkpoints unmasks the ability of drugs to cause immune mediated liver injury (Mak and Uetrecht, 2015). We used nevirapine in this study because it is associated with a significant risk of both serious skin rash and idiosyncratic liver injury in humans, which limits its use (FDA, 2011; Tseng *et al.*, 2014). Nevirapine also causes sex- and strain-dependent skin rash in rats, but not in mice (Shenton *et al.*, 2003), and mild liver injury in PD-$1^{-/-}$ mice cotreated with anti-CTLA-4 (Mak and Uetrecht, 2015).

In the current study, nevirapine produced serious liver injury in the PD-$1^{m/m}$ rats. The marked increase in CD8+ T cells in the liver and blood (Figure 5) strongly suggests that the liver injury is mediated principally by cytotoxic T cells, although there was also an increase in NK cells in the blood. In contrast, there was a decrease in CD4+ T cells and B cells. There was also a marked increase in inflammatory cytokine and chemokine mRNA in the liver, with a decrease in IL-10 relative to WT rats treated with

Downloaded from https://academic.oup.com/toxsci/advance-article/doi/10.1093/toxsci/kfae058/7674865 by UNIV OF TORONTO SCARBOROUGH LIBRARY user on 27 May 2024

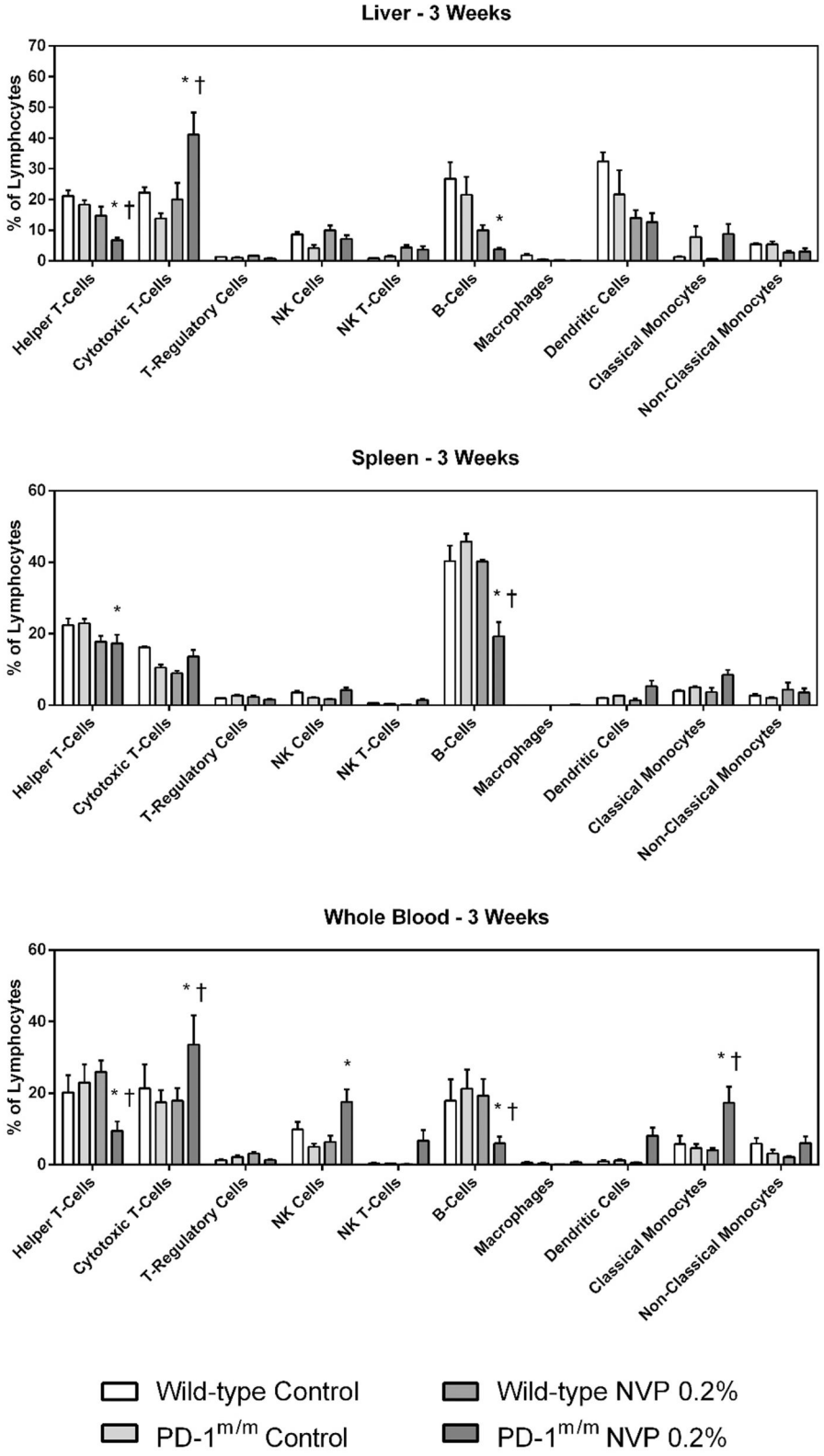

Figure 5. Populations of different leukocytes between control and nevirapine (NVP)-treated wild-type and PD-$1^{m/m}$ females in the liver, spleen, and blood at day 21. An increase in cytotoxic T-cells and a relative decrease in T-helper cells and B-cells were observed in the liver of the nevirapine-treated PD-$1^{m/m}$ females when compared with control PD-$1^{m/m}$ or nevirapine-treated wild-type females. In the spleen, relative decreases in helper T-cells and B-cells were observed in the nevirapine-treated PD-$1^{m/m}$ females. Increases in cytotoxic T-cells, NK cells, and classical monocytes with a decrease in T-helper cells and B-cells were detected in the blood of the nevirapine-treated PD-$1^{m/m}$ females. Data show the percentage of each cell population from the total population of gated leukocytes. The data represent the mean ± SEM, and statistical significance was tested using a 2-way ANOVA with Tukey's multiple comparisons test ($n = 3$–6 per group), * $p < .05$ for treatment-mediated effects (same genotype, different treatment); † $p < .05$ for genotype-mediated effects between wild-type and PD-$1^{m/m}$ animals (same treatment, different genotype).

Downloaded from https://academic.oup.com/toxsci/advance-article/doi/10.1093/toxsci/kfae058/7674865 by UNIV OF TORONTO SCARBOROUGH LIBRARY user on 27 May 2024

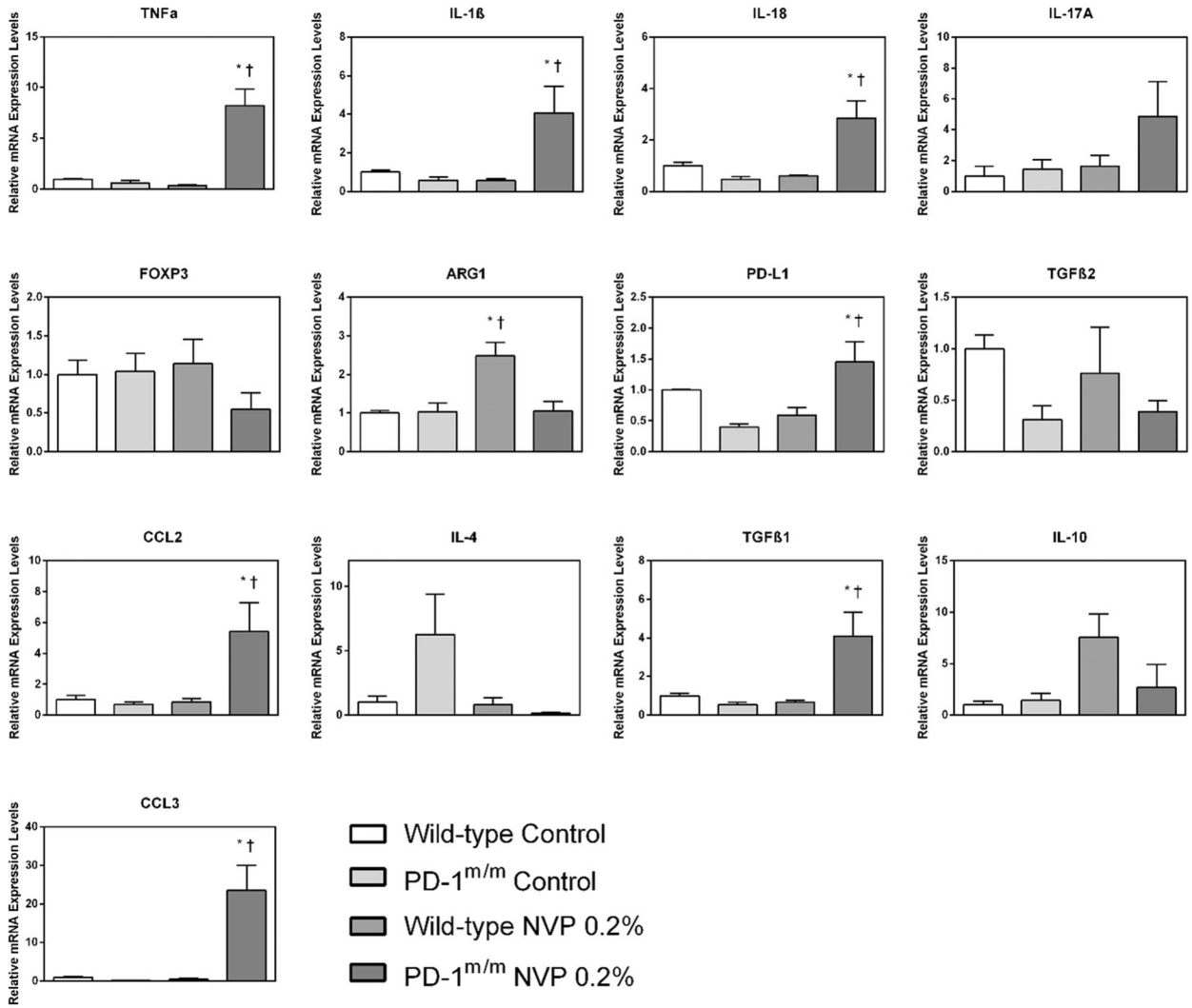

Figure 6. Gene expression changes in the liver of control and nevirapine (NVP)-treated wild-type and PD-1$^{m/m}$ females at endpoint (day 21). Primer sequences utilized are presented in Supplementary Table 1. Significant increases were observed in TNFα, IL-1β, IL-18, CCL2, CCL3, TGFβ1, and PD-L1 transcript levels in the nevirapine-treated PD-1$^{m/m}$ females. An increase in ARG1 mRNA was also noted in the nevirapine-treated wild-type females in comparison with all other groups. Data were normalized to wild-type control animals and fold changes were computed by the comparative cycle threshold (ΔΔCT) method. The data represent the mean ± SEM, and statistical significance was tested using a 2-way ANOVA with Tukey's multiple comparisons test ($n = 3$ per group), * $p < .05$ for treatment-mediated effects (same genotype, different treatment); † $p < .05$ for genotype-mediated effects between wild-type and PD-1$^{m/m}$ animals (same treatment, different genotype).

nevirapine (Figure 6). Again, this is clear evidence of an inflammatory immune reaction. There was an increase in PD-L1 mRNA, presumably in response to the decrease in intact PD-1.

We expected that the skin rash caused by nevirapine in rats would be more severe in PD-1$^{m/m}$ animals; however, that was not the case. It may be that impairing immune tolerance only increases the risk of liver injury. It is true that immune tolerance is more important in the liver than in the skin, presumably because the liver is exposed to so many "foreign" and inflammatory molecules from the intestine. However, immune checkpoint inhibitors can cause skin rashes in humans (Callahan and Wolchok, 2013), so it is surprising that the PD-1$^{m/m}$ rats did not develop a skin rash. It is important to note that the skin rash caused by nevirapine in Brown Norway rats is mediated by CD4$^+$ T cells (Shenton *et al.*, 2005), and the elimination of PD-1 promotes a CD8 T cell immune response as shown in these experiments. This is the most likely reason that the PD-1$^{m/m}$ rats did not develop a skin rash. We were not even able to reproduce the low incidence (approximately 20%) of the skin rash that we had previously observed in wild-type female Sprague Dawley rats. It is not clear what changed in the 17 years since that original observation (Shenton *et al.*, 2003). The number of animals treated was relatively small, and it is likely just be a matter of probability. Although the wild-type rats were bred in-house, they were derived from rats from Charles River, which was the source of the animals in the earlier study. We conducted a small study with Sprague Dawley rats obtained directly from Charles River, but again, they did not develop a rash (data not shown). Although we did not measure covalent binding in the skin of these rats, we have previously demonstrated covalent binding of nevirapine in the skin of rats (Sharma *et al.*, 2013a,b), rats are known to express sulfotransferases in the skin (Oesch *et al.*, 2007), and it is very unlikely that the genetic change in PD-1 would affect expression of sulfotransferases. Another factor is that, unlike Brown Norway rats, Sprague Dawley rats are outbred. The rash in female Brown Norway rats has been replicated

Downloaded from https://academic.oup.com/toxsci/advance-article/doi/10.1093/toxsci/kfae058/7674865 by UNIV OF TORONTO SCARBOROUGH LIBRARY user on 27 May 2024

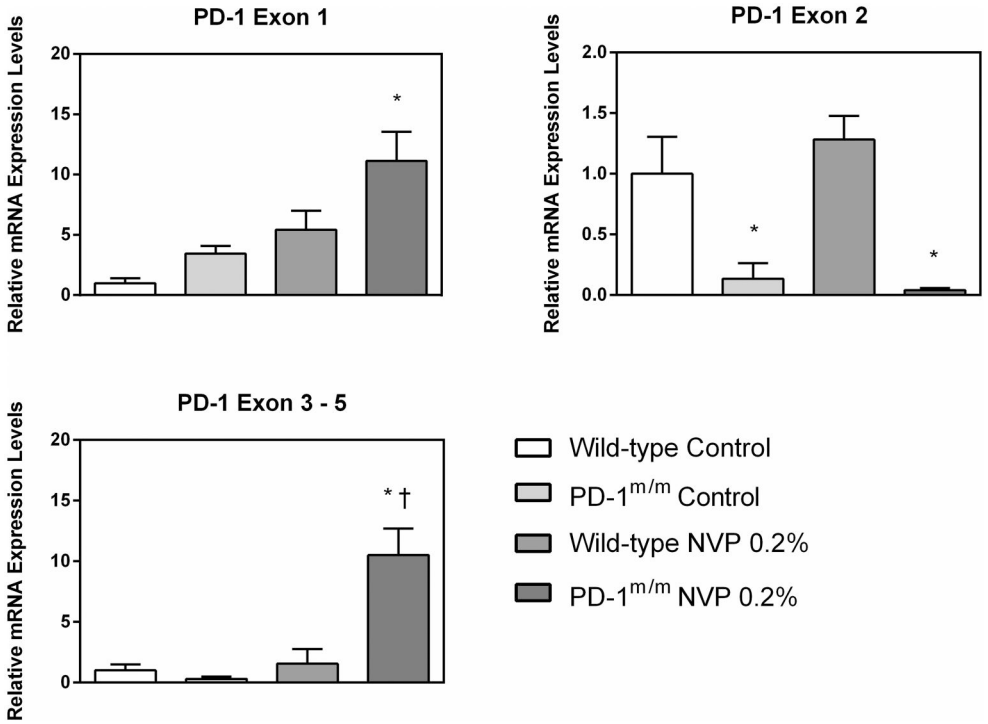

Figure 7. Modification of PD-1 exon 2 alters the natural pattern of exon utilization, both intrinsically and under stress. Primer sequences utilized are presented in Supplementary Table 2. Data represent the mean ± SEM, with statistical significance tested by 2-way ANOVA with Tukey's multiple comparisons test ($n = 3$ per group), * $p < .05$ for treatment-mediated effects (same genotype, different treatment); † $p < .05$ for genotype-mediated effects between wild-type and PD-$1^{m/m}$ animals (same treatment, different genotype).

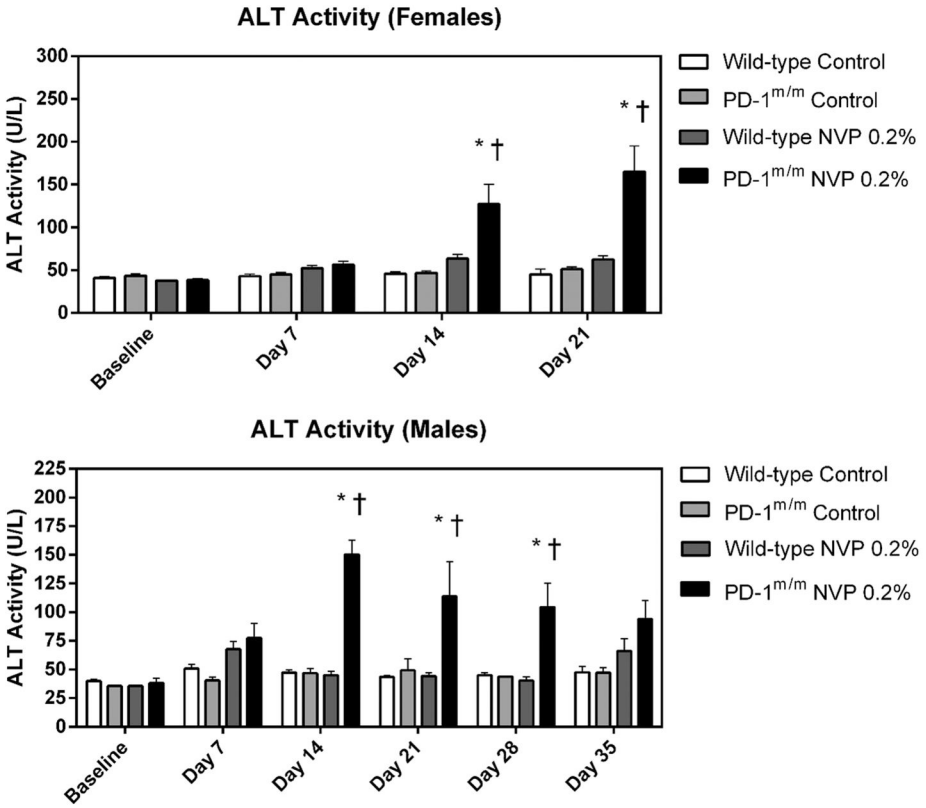

Figure 8. Serum ALT activity levels of control and nevirapine (NVP)-treated female and male rats. Significantly elevated ALT levels were observed on day 14 and day 21 in the nevirapine-treated PD-$1^{m/m}$ females. Significantly elevated ALT levels were measured on day 14, day 21, and day 28 in the nevirapine-treated PD-$1^{m/m}$ males. No significant differences were detected at endpoint in male animals. The data represent the mean ± SEM, and statistical significance was tested using a 2-way ANOVA with Tukey's multiple comparisons test ($n = 3$–15 per group), * $p < .05$ for treatment-mediated effects (same genotype, different treatment); † $p < .05$ for genotype-mediated effects between wild-type and PD-$1^{m/m}$ animals (same treatment, different genotype).

Downloaded from https://academic.oup.com/toxsci/advance-article/doi/10.1093/toxsci/kfae058/7674865 by UNIV OF TORONTO SCARBOROUGH LIBRARY user on 27 May 2024

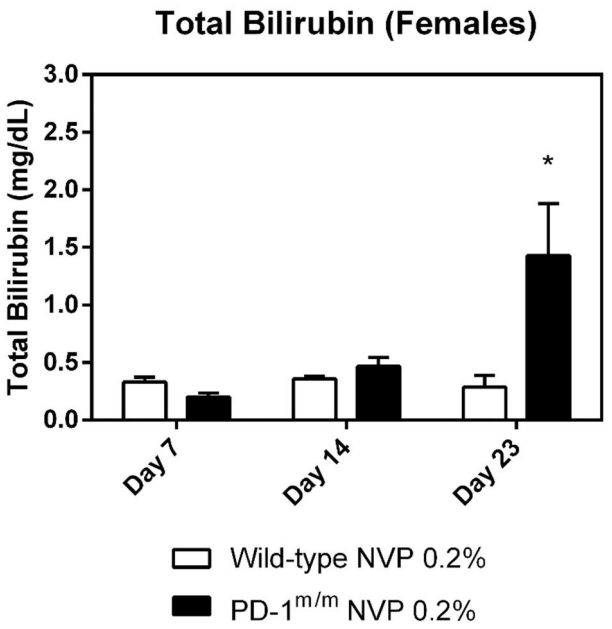

Figure 9. Total serum bilirubin of nevirapine (NVP)-treated wild-type and PD-$1^{m/m}$ female rats. Nevirapine-treated PD-$1^{m/m}$ animals have a significantly greater level of total serum bilirubin compared with nevirapine-treated wild-type animals at day 23 (week 3). The data represent the mean ± SEM, and statistical significance was tested using a 2-way ANOVA with Tukey's multiple comparisons test ($n = 3$ per group), * $p < .05$ for treatment-mediated effects (same genotype, different treatment).

many times so we are confident that Brown Norway rats do develop a rash when treated with nevirapine. It would be interesting to develop a PD-$1^{-/-}$ Brown Norway rat, but that would be a significant undertaking.

Although treatment of PD-$1^{m/m}$ rats with nevirapine did not lead to a skin rash, it clearly did produce a marked immune response and resulted in significant liver injury with increases in inflammatory cytokines and chemokines for the recruitment and activation of polymorphonuclear leukocytes. The PD-$1^{m/m}$ rats had a more severe immune response to nevirapine than PD-$1^{-/-}$ mice even though the mice were also treated with anti-CTLA-4. The liver injury was also more severe; although the ALT was not much higher, the histology showed much more hepatic necrosis, and there was an increase in bilirubin and a decrease in serum cholesterol indicating a decrease in liver function presumably due to the reduced liver lipoprotein biosynthesis (Ghadir *et al.*, 2010; Sanne *et al.*, 2005). The modest increase in ALT relative to the histology and functional changes is likely due in part to the fact that this is chronic liver injury rather than acute injury. As in humans, the injury was greater in females than males.

Overall, immune tolerance may be more crucial for immune-mediated liver injury than for skin rashes. In the previous study with amodiaquine, liver injury occurred in the PD-$1^{m/m}$ rats, but agranulocytosis did not even though amodiaquine can cause immune-mediated agranulocytosis in humans (Cho *et al.*, 2024). This study highlights the complexity of the immune response to drugs. The observation that we no longer saw a skin rash in Sprague Dawley rats emphasizes the idiosyncratic nature of IDRs where small factors may tip the balance and determine the outcome of an immune response. Given the difficulty of performing such controlled studies in humans, it is important to study the immune response to drugs in animals. Even though there are clearly differences in the immune response between humans and rodents, there are also differences between how different individuals in the same species respond, and Jim Gillette once said that a specific rat may be a better model for a specific human than another human.

Supplementary data

Supplementary data are available at *Toxicological Sciences* online.

Declaration of conflicting interests

The authors declared no potential conflicts of interest with respect to the research, authorship, and/or publication of this article.

Funding

Cas9-derived rat production was funded by the Government of Canada through Genome Canada and Ontario Genomics (OGI-099). The project was funded by Canadian Institutes of Health Research (178188); Pfizer Canada; the Ontario Graduate Scholarship; and the Glaxo-Wellcome Sunnybrook Drug Safety Clinic Graduate Student Fellowship.

Acknowledgments

The authors wish to acknowledge the contribution of Dr Andrew Elia and Dr Lily Zhou at the Princess Margaret Hospital/University Health Network for their histology services and knowledge; Beth Binnington from the Canadian Blood Services for consultation and assistance; Dr Nitin Bhardwaj for necropsies at the Division of Comparative Medicine, University of Toronto; Brittany Licorish, Laura Kent, and Stacy Nichols for care and maintenance of the genetically modified rat colony at the Division of Comparative Medicine, University of Toronto; and Kyra Alam for her guidance and support. The authors also wish to acknowledge the contribution of the Model Production Core staff at The Centre for Phenogenomics for the generation of genetically modified rat model.

References

Ahn, E., Araki, K., Hashimoto, M., Li, W., Riley, J. L., Cheung, J., Sharpe, A. H., Freeman, G. J., Irving, B. A., and Ahmed, R. (2018). Role of PD-1 during effector CD8 T cell differentiation. *Proc. Natl. Acad. Sci. U.S.A.* **115**, 4749–4754.

Almond, L. M., Boffito, M., Hoggard, P. G., Bonora, S., Raiteri, R., Reynolds, H. E., Garazzino, S., Sinicco, A., Khoo, S. H., Back, D. J., *et al.* (2004). The relationship between nevirapine plasma concentrations and abnormal liver function tests. *AIDS Res. Hum. Retroviruses* **20**, 716–722.

Bersoff-Matcha, S. J., Miller, W. C., Aberg, J. A., van Der Horst, C., Hamrick, H. J., Jr, Powderly, W. G., and Mundy, L. M. (2001). Sex differences in nevirapine rash. *Clin. Infect. Dis.* **32**, 124–129.

Callahan, M. K., and Wolchok, J. D. (2013). At the bedside: CTLA-4- and PD-1-blocking antibodies in cancer immunotherapy. *J. Leukoc. Biol.* **94**, 41–53.

Chen, J., Mannargudi, B. M., Xu, L., and Uetrecht, J. (2008). Demonstration of the metabolic pathway responsible for nevirapine-induced skin rash. *Chem. Res. Toxicol.* **21**, 1862–1870.

Downloaded from https://academic.oup.com/toxsci/advance-article/doi/10.1093/toxsci/kfae058/7674865 by UNIV OF TORONTO SCARBOROUGH LIBRARY user on 27 May 2024

Cho, T., and Uetrecht, J. (2017). How reactive metabolites induce an immune response that sometimes leads to an idiosyncratic drug reaction. *Chem. Res. Toxicol.* **30**, 295–314.

Cho, T., Wierk, A., Gertsenstein, M., Rodgers, C., Uetrecht, J., and Henderson, J. T. (2024). The development and characterization of a CRISPR/Cas9-mediated PD-1 functional knockout rat as a tool to study idiosyncratic drug reactions. *Toxicol. Sci.* **198**, 233–245.

Chrostek, L., Supronowicz, L., Panasiuk, A., Cylwik, B., Gruszewska, E., and Flisiak, R. (2014). The effect of the severity of liver s on the level of lipids and lipoproteins. *Clin. Exp. Med.* **14**, 417–421.

DrugBank. 2023. (2023). nevirapine. Available at: https://go.Drugbank.Com/drugs/db00238. Date accessed October 2023.

Food and Drug Administration [FDA] (2011). Prescribing information for Viramune. Available at: https://www.Accessdata.Fda.Gov/drugsatfda_docs/label/2011/020636s039_020933s030lbl.Pdf. Date accessed November 2011.

Friedmann, P. S., Strickland, I., Pirmohamed, M., and Park, B. K. (1994). Investigation of mechanisms in toxic epidermal necrolysis induced by carbamazepine. *Arch. Dermatol.* **130**, 598–604.

Ghadir, M. R., Riahin, A. A., Havaspour, A., Nooranipour, M., and Habibinejad, A. A. (2010). The relationship between lipid profile and severity of liver damage in cirrhotic patients. *Hepat Mon* **10**, 285–288.

Jee, A., Sernoskie, S. C., and Uetrecht, J. (2021). Idiosyncratic drug-induced liver injury: Mechanistic and clinical challenges. *Int. J. Mol. Sci.* **22**, 2954.

Mak, A., and Uetrecht, J. (2015). The combination of anti-CTLA-4 and $PD1^{-/-}$ mice unmasks the potential of isoniazid and nevirapine to cause liver injury. *Chem. Res. Toxicol.* **28**, 2287–2291.

Metushi, I. G., Hayes, M. A., and Uetrecht, J. (2015). Treatment of PD-1(−/−) mice with amodiaquine and anti-CTLA4 leads to liver injury similar to idiosyncratic liver injury in patients. *Hepatology* **61**, 1332–1342.

Nassif, A., Bensussan, A., Boumsell, L., Deniaud, A., Moslehi, H., Wolkenstein, P., Bagot, M., and Roujeau, J. C. (2004). Toxic epidermal necrolysis: Effector cells are drug-specific cytotoxic T cells. *J. Allergy Clin. Immunol.* **114**, 1209–1215.

Nielsen, C., Ohm-Laursen, L., Barington, T., Husby, S., and Lillevang, S. T. (2005). Alternative splice variants of the human PD-1 gene. *Cell. Immunol.* **235**, 109–116.

Oesch, F., Fabian, E., Oesch-Bartlomowicz, B., Werner, C., and Landsiedel, R. (2007). Drug-metabolizing enzymes in the skin of man, rat, and pig. *Drug Metab. Rev.* **39**, 659–698.

Ribas, A., Hodi, F. S., Callahan, M., Konto, C., and Wolchok, J. (2013). Hepatotoxicity with combination of vemurafenib and ipilimumab. *N. Engl. J. Med.* **368**, 1365–1366.

Sanne, I., Mommeja-Marin, H., Hinkle, J., Bartlett, J. A., Lederman, M. M., Maartens, G., Wakeford, C., Shaw, A., Quinn, J., Gish, R. G., *et al.* (2005). Severe hepatotoxicity associated with nevirapine use in HIV-infected subjects. *J. Infect. Dis.* **191**, 825–829.

Sernoskie, S. C., Jee, A., and Uetrecht, J. P. (2021). The emerging role of the innate immune response in idiosyncratic drug reactions. *Pharmacol. Rev.* **73**, 861–896.

Sharma, A. M., Klarskov, K., and Uetrecht, J. (2013a). Nevirapine bioactivation and covalent binding in the skin. *Chem. Res. Toxicol.* **26**, 410–421.

Sharma, A. M., Novalen, M., Tanino, T., and Uetrecht, J. P. (2013b). 12-OH-Nevirapine sulfate, formed in the skin, is responsible for nevirapine-induced skin rash. *Chem. Res. Toxicol.* **26**, 817–827.

Shenton, J. M., Popovic, M., Chen, J., Masson, M. J., and Uetrecht, J. P. (2005). Evidence of an immune-mediated mechanism for an idiosyncratic nevirapine-induced reaction in the female Brown Norway rat. *Chem. Res. Toxicol.* **18**, 1799–1813.

Shenton, J. M., Teranishi, M., Abu-Asab, M. S., Yager, J. A., and Uetrecht, J. P. (2003). Characterization of a potential animal model of an idiosyncratic drug reaction: Nevirapine-induced skin rash in the rat. *Chem. Res. Toxicol.* **16**, 1078–1089.

Tseng, Y. T., Yang, C. J., Chang, S. Y., Lin, S. W., Tsai, M. S., Liu, W. C., Wu, P. Y., Su, Y. C., Luo, Y. Z., Yang, S. P., *et al.* (2014). Incidence and risk factors of skin rashes and hepatotoxicity in HIV-infected patients receiving nevirapine-containing combination antiretroviral therapy in Taiwan. *Int. J. Infect. Dis.* **29**, 12–17.

Uetrecht, J. (2019). Mechanistic studies of idiosyncratic Dili: Clinical implications. *Front. Pharmacol.* **10**, 837.

Uetrecht, J., and Naisbitt, D. J. (2013). Idiosyncratic adverse drug reactions: Current concepts. *Pharmacol. Rev.* **65**, 779–808.

White, T. J., Arakelian, A., and Rho, J. P. (1999). Counting the costs of drug-related adverse events. *Pharmacoeconomics.* **15**, 445–458.

Zhang, Q., Fu, Y., Thakur, C., Bi, Z., Wadgaonkar, P., Qiu, Y., Xu, L., Rice, M., Zhang, W., Almutairy, B., *et al.* (2020). CRISPR-Cas9 gene editing causes alternative splicing of the targeting mRNA. *Biochem. Biophys. Res. Commun.* **528**, 54–61.

© The Author(s) 2024. Published by Oxford University Press on behalf of the Society of Toxicology.
All rights reserved. For permissions, please e-mail: journals.permissions@oup.com
Toxicological Sciences, 2024, 00, 1–12
https://doi.org/10.1093/toxsci/kfae058
Research article

Downloaded from https://academic.oup.com/toxsci/advance-article/doi/10.1093/toxsci/kfae058/7674865 by UNIV OF TORONTO SCARBOROUGH LIBRARY user on 27 May 2024